Surface structures of ternary iron arsenides $A\mathrm{Fe_2As_2}$ (A = Ba, Sr, or Ca)

Miao Gao,[1] Fengjie Ma,[1,2] Zhong-Yi Lu,[1,*] and Tao Xiang[3,2,†]
[1]*Department of Physics, Renmin University of China, Beijing 100872, China*
[2]*Institute of Theoretical Physics, Chinese Academy of Sciences, P.O. Box 2735, Beijing 100190, China*
[3]*Institute of Physics, Chinese Academy of Sciences, P.O. Box 603, Beijing 100190, China*
(Received 23 March 2010; revised manuscript received 18 April 2010; published 19 May 2010)

By the first-principles electronic structure calculations, we find that energetically the most favorable cleaved $A\mathrm{Fe_2As_2}(001)$ surface is A-terminated with either $\sqrt{2}\times\sqrt{2}$ or 1×2 order. For $\mathrm{BaFe_2As_2}$, the surface Ba atoms are predominantly in a $\sqrt{2}\times\sqrt{2}$ order. A low-temperature cleaving may generate a metastable As-terminated surface. The As-terminated surface in the antiferromagnetic orthorhombic $\mathrm{BaFe_2As_2}$ also takes a $\sqrt{2}\times\sqrt{2}$ order, resulting from the buckling of the surface As atoms and giving rise to a switchable $\sqrt{2}\times\sqrt{2}$ scanning tunneling microscopy (STM) pattern upon varying the applied bias. In a 1×2-ordered A-terminated surface, the high-density spots in the STM image do not directly correspond to the positions of surface atoms. Our results are consistent with the STM observations and resolve the discrepancy between different experimental groups. The study helps establish a physical picture to understand the cleaved $A\mathrm{Fe_2As_2}$ surfaces.

DOI: 10.1103/PhysRevB.81.193409 PACS number(s): 68.35.B−, 68.43.Bc, 73.20.−r, 74.70.Dd

Recently great interest has been devoted to the investigation of the iron-based superconductor compounds[1,2] because they have not only reached the second highest superconductivity temperatures but also broken conventional wisdom that magnetic Fe ions are pair breakers of superconductivity. Among these compounds, the ternary iron arsenides are most investigated because there are the high-quality single crystals available. Both neutron-scattering measurements and theoretical studies have revealed that the undoped parent compounds are in either collinear or bicollinear antiferromagnetic (AFM) order below either tetragonal-orthorhombic or tetragonal-triclinic structural transition temperature.[3–5]

The surfaces of high-quality $\mathrm{BaFe_2As_2}$ and $\mathrm{SrFe_2As_2}$ single crystals have been probed by scanning tunneling microscopy (STM).[6–10] However, the contradictory experimental observations on the surface structures have been reported. On a single crystal of $\mathrm{BaFe_2As_2}$ cleaved at 20 K, the STM images observed at 4.3 K showed a dominant $\sqrt{2}\times\sqrt{2}$ order, which was interpreted as due to the ordering of As atoms on the terminated surface.[7] The STM measurement on another $\mathrm{BaFe_2As_2}$ single crystal, cleaved at 120 K also revealed a $\sqrt{2}\times\sqrt{2}$ order, but it was interpreted as due to the ordering of Ba atoms on the terminated surface.[8] Meanwhile, it was also reported that the cleaved surface of $\mathrm{BaFe_2As_2}$ exhibit a complex diversity of ordered and disordered structures depending on the cleaving temperature.[9] On the other hand, the STM measurement observed both $\sqrt{2}\times\sqrt{2}$ and 1×2 orders on the surface of a $\mathrm{SrFe_2As_2}$ single crystal.[10] All of these reflect that there are rich surface properties distinct from the bulk. A thorough investigation on the underlying atomic and electronic structures of the cleaved surfaces in iron pnictides is important to resolve the above contradictory observations and to great potential surface-based applications as well. This is also important to the understanding of experimental data measured by other surface-sensitive probes such as angle-resolved photoemission spectroscopy (ARPES), which is unique in directly determining the electronic structures of crystals.

Here we present the results of first-principles electronic structure calculations on the (001) surfaces of $A\mathrm{Fe_2As_2}$ (denoted as $A122$). We find that the A-terminated surface with $\sqrt{2}\times\sqrt{2}$ or 1×2 order is energetically most favorable in both nonmagnetic (NM) tetragonal and AFM orthorhombic phases. Cleaving at very low temperatures may lift A atoms free in a large area, resulting in an ordered As layer to expose on the surface. Correspondingly, there are surface electronic states induced crossing the Fermi energy. These surface structures lead to different STM patterns and affect strongly the low energy electronic structures of the compounds.

In our calculations the plane-wave basis method was used.[11,12] We adopted the generalized gradient approximation of Perdew-Burke-Ernzerhof[13] for the exchange-correlation potentials. The ultrasoft pseudopotentials[14] were used to model the electron-ion interactions. To study the magnetic structures and properties, the calculations were fully spin-polarized and unrestricted. After the full convergence test, the kinetic-energy cutoff and the charge-density cutoff of the plane-wave basis were chosen to be 408 and 4082 eV, respectively. The Gaussian broadening technique was used and a mesh of 16×16 k points was sampled for the 1×1 irreducible surface Brillouin-zone integration. We modeled a surface using a slab of six FeAs layers and five or seven A layers plus a vacuum layer of 20–25 Å with inversion symmetry through the center of the slab. We froze the two innermost middle FeAs layers with one A layer in relaxation. The experimental lattice constants were adopted.

In A122 compounds, As or A atoms within each own layer form a square lattice with ~4 Å periodicity in the bulk. A unit cell of this square lattice is thus about 4 Å×4 Å. In this paper, we define a surface unit cell in reference to such a square lattice. After cleaving, the surface can terminate at either an A-atom layer or an As-atom layer since an Fe-atom layer will not expose on surface due to the strong chemical bonding between Fe and As ions. For A termination, half of A atoms should remain on the surface as uniformly as possible to balance the chemical valence. The order that the A atoms can take is either $\sqrt{2}\times\sqrt{2}$ or 1×2, derived by half of A atoms being removed alternatively from the original 1

TABLE I. Relative energies of two $\sqrt{2}\times\sqrt{2}$ A-terminated surfaces and two 1×2 A-terminated surfaces with respect to a 1×1 A-terminated plus a 1×1 As-terminated surfaces in the NM tetragonal phase and the AFM orthorhombic phase, respectively. The energy unit is meV/$(1\times1$ cell). Here the surface atoms are set in the corresponding bulk positions. Considering reconstruction, only As-terminated surface takes further reconstruction with a very small energy gain of ~3.9 meV/$(1\times1$ cell).

AFe_2As_2 (001)	NM tetragonal		AFM orthorhombic	
	$2\times(\sqrt{2}\times\sqrt{2})$	$2\times(1\times2)$	$2\times(\sqrt{2}\times\sqrt{2})$	$2\times(1\times2)$
$BaFe_2As_2$	−411.6	−217.8	−534.8	−312.0
$SrFe_2As_2$	−217.0	−167.8	−314.6	−219.0
$CaFe_2As_2$	−34.0	−97.0	−185.4	−189.2

$\times1$ square lattice along the square-diagonal or square-side direction before further possible reconstruction. For ideal (unreconstructed) As termination, the As atoms are in 1×1 order. In the following paragraphs we will show actually only As-terminated surface takes further reconstruction with a very small energy gain of ~3.9 meV/$(1\times1$ cell). A realistic cleaved surface will consist mainly of these orders with certain disorders, which is too complex to do theoretical study. To simplify the problem in physics, cleaving is considered to immediately generate two ordered surfaces with the surface atoms in the corresponding bulk positions. It turns out that there are three possible ordered surface structures immediately generated after cleaving, namely, two $\sqrt{2}\times\sqrt{2}$ A-terminated surfaces, two 1×2 A-terminated surfaces, or a 1×1 As-terminated surface accompanied with a 1×1 A-terminated surface, respectively.

Table I shows the relative energies among the three possible ordered cleaved structures in the NM tetragonal and the AFM orthorhombic phases, respectively. We find that the A-terminated surfaces with $\sqrt{2}\times\sqrt{2}$ or 1×2 order have always much lower energy than the 1×1 A-terminated plus the 1×1 As-terminated surfaces in both NM and AFM cases. Specifically, energetically the most favorable cleaved surface is $\sqrt{2}\times\sqrt{2}$-ordered in Ba122 and Sr122, and 1×2-ordered in Ca122, respectively. For both Sr122 and Ca122 compounds, the energy difference between these two kinds of A-terminated surfaces is small. This suggests that it will have higher probability to observe both $\sqrt{2}\times\sqrt{2}$ and 1×2 ordered structures on the same cleaved surface for these two compounds.

Besides considering energetically above, the cleaved surfaces are substantially affected by the cleaving process itself, i.e., the energy barriers in a cleaving process. A realistic cleaving process is again too complex to simulate theoretically. We design an ideal adiabatic cleaving process, in which a sample is divided into two parts by separating two neighbor FeAs layers gradually away from each other. The in-between A layer is either divided half by half into each of the FeAs layers or kept as a whole in one of FeAs layers in the separation process. The idea is the same as the one used in thermodynamics to study the entropy effect. It turns out that no significant separation barrier energies are found in all the processes. This suggests that the energetics shown in Table I can well describe the cleaved surfaces.

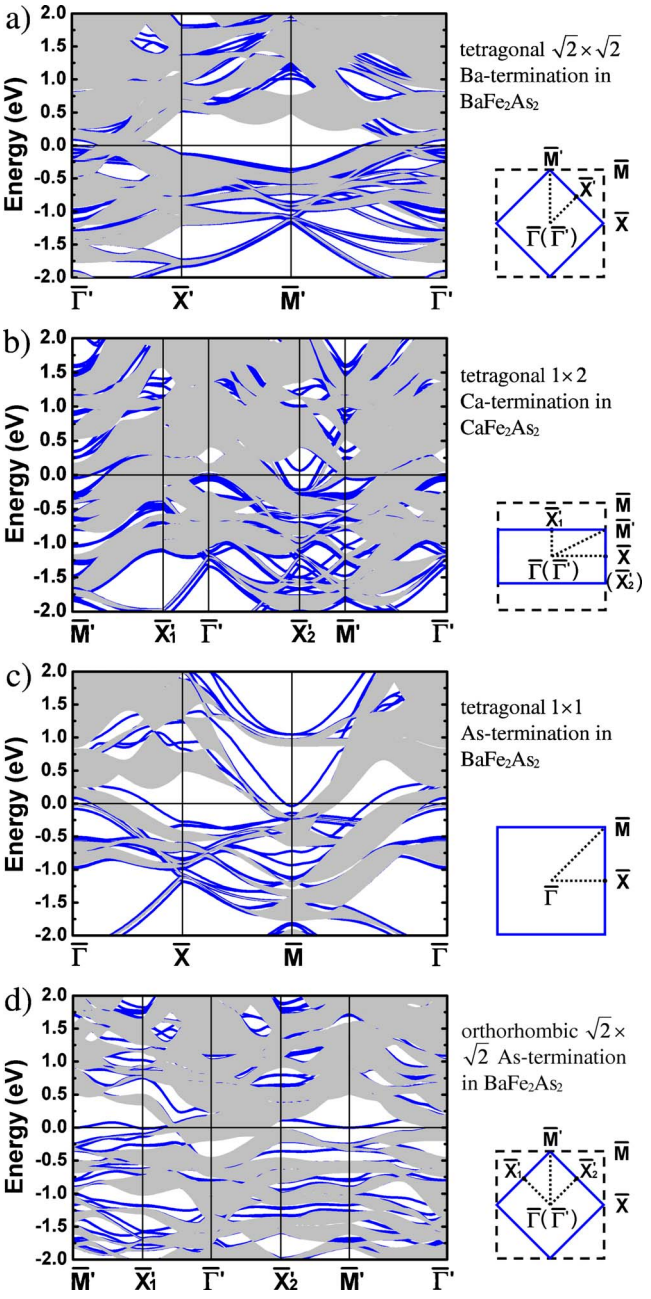

FIG. 1. (Color online) Calculated surface electronic band structures of AFe_2As_2 (A=Ba, Sr, or Ca) (001) surface reported along the high-symmetry lines of the irreducible surface Brillouin zone for (a) nonmagnetic $\sqrt{2}\times\sqrt{2}$ Ba-terminated Ba122 surface; (b) nonmagnetic 1×2 Ca-terminated Ca122 surface; (c) nonmagnetic 1×1 As-terminated $BaFe_2As_2$ surface; (d) antiferromagnetic $\sqrt{2}\times\sqrt{2}$ As-terminated $BaFe_2As_2$ surface, respectively. The Fermi level is set to zero. The shaded areas correspond to the surface-projected bulk states while solid curves correspond to the surface states. The surface Brillouin zone is shown next to each band-structure plot. The dashed squares are 1×1 surface Brillouin zones. The 1×1 surface Brillouin zone is folded in (a), (b), and (d).

For the "$\sqrt{2}\times\sqrt{2}$" A termination, our calculation shows that there is no further buckling or dimerization except small

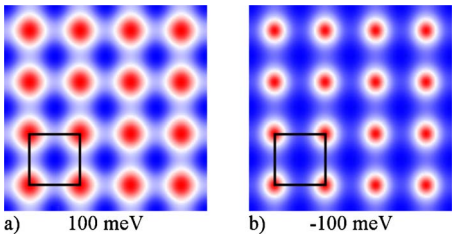

FIG. 2. (Color online) Simulated STM images of the $\sqrt{2}\times\sqrt{2}$ Ba-terminated $BaFe_2As_2$ surface in the antiferromagnetic orthorhombic phase with bias voltages of (a) 100 and (b) −100 meV. The black squares indicate the $\sqrt{2}\times\sqrt{2}$ surface unit cells. Similar STM images are obtained for the $\sqrt{2}\times\sqrt{2}$ Sr(Ca)-terminated $Sr(Ca)Fe_2As_2$ surface.

relaxation on surface in both NM tetragonal and AFM orthorhombic phases. Since the chemical valence is well balanced in the surface layer, it is expected that no corresponding surface states will cross the Fermi level. This is verified by our surface band-structure calculations [Fig. 1(a)]. The surface states are found only around the edges of the bulk energy-gap regions, induced by the reduced surface symmetry. But there is the Brillouin-zone folding effect, namely, the 1×1 surface Brillouin zone is reduced by half through folding in the $\sqrt{2}\times\sqrt{2}$ surface Brillouin zone. As shown in Fig. 1(a), tetragonal $\bar{M}$ and $\bar{\Gamma}$ become $\bar{\Gamma}'$ in the folded Brillouin zone, and tetragonal $\bar{X}$ is now located at $\bar{M}'$. The calculated STM images all show a $\sqrt{2}\times\sqrt{2}$ order in both NM tetragonal and AFM orthorhombic phases (Fig. 2), in agreement with the recent STM observation.[8]

For the "1×2" A termination, no any further lattice reconstruction (buckling or dimerization) is found for the surface A atoms either. However, in both NM tetragonal and AFM orthorhombic phases, the surface A atoms move downward and force the As atoms just below the surface layer to dimerize toward each other by ~0.05 Å. This small dimerization occurs in the direction perpendicular to the surface A atom row and is located in the troughs between the A atom rows as shown in Fig. 3. This leads to some surface states near the Fermi energy [Fig. 1(b)]. The high-density spots of the STM images obtained from our calculation appear along the A atom rows, but not directly on the top of A atoms (Fig. 3). Thus the brightest spots of the STM image do not correspond to the positions of the surface A atoms. This unusual STM pattern is due to the hybridization between the surface A atoms and As atoms. This leads to a natural explanation why the STM image observed in Sr122 looks as in a 1×2 dimerized As-terminated surface,[10] although the true surface is 1×2 Sr terminated.

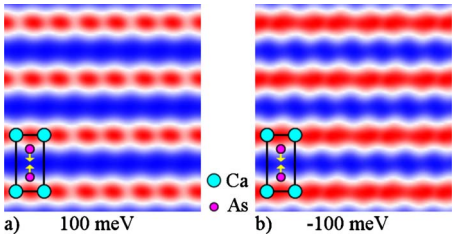

FIG. 3. (Color online) Simulated STM images of the 1×2 Ca-terminated $CaFe_2As_2$ surface in the antiferromagnetic orthorhombic phase with bias voltages of (a) 100 and (b) −100 meV. The rectangles indicate 1×2 surface unit cells. Note that the bright spots do not directly correspond to the positions of surface atoms. Similar STM images are obtained for the 1×2 Ba(Sr)-terminated $Ba(Sr)Fe_2As_2$ surface.

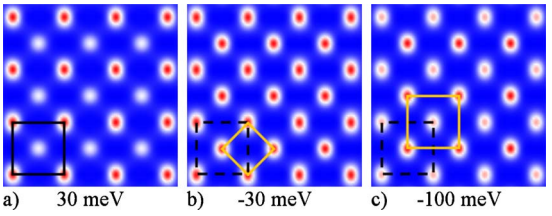

FIG. 4. (Color online) Simulated STM images of the $\sqrt{2}\times\sqrt{2}$ As-terminated $BaFe_2As_2$ surface in the AFM orthorhombic phase with bias voltages of (a) 30, (b) −30, and (c) −100 meV. The large squares represent the $\sqrt{2}\times\sqrt{2}$ surface unit cells. The small diamond represents a 1×1 surface unit cell. The simulated STM images for As-terminated $Sr(Ca)Fe_2As_2$ surface show a 1×1 order similar to (b).

Realistically, a fast cleaving may readily remove the order of A atoms on the surface and yield a metastable As-terminated surface with randomly assembled A atoms, as suggested by the experiment.[7] If the cleaving is done at very low temperature, this metastable structure can remain on the surface for a long time although the energy barriers to move these A atoms back to the equilibrium positions are found to be only a few tenths of eV by the calculations. The low energy electronic structure is expected to be strongly modified since the unbalanced chemical valence in the surface FeAs layer will induce surface states crossing the Fermi energy. This may further induce surface reconstruction through buckling or dimerization of the surface As atoms.

In the nonmagnetic tetragonal phase of $A122$, for all the As terminations, we do not find any surface reconstruction like buckling or dimerization. But the low-lying electronic structure is strongly modified due to the imbalance of chemical valence on surface. Especially there are partially filled surface states crossing the Fermi energy [Fig. 1(c)], which may show some Fermi-surface arcs, larger or smaller than the bulk ones, in ARPES. The simulated STM images all show a 1×1 order, similar to Fig. 4(b).

In the antiferromagnetic orthorhombic phase, for the As-terminated Ba122 surface a small buckling of ~0.1 Å occurs with an energy gain of ~3.9 meV/(1×1 cell). Such a small buckling can nevertheless affect strongly the STM measurement, as shown in Fig. 4. For a positive bias or a small negative bias [Fig. 4(a)], the calculated STM image shows a $\sqrt{2}\times\sqrt{2}$ order, in which the buckled inward As atoms show strong bright spots while the buckled outward As atoms are almost invisible. When the applied bias is between −30 and −50 meV [Fig. 4(b)], a 1×1 order of bright spots is found, in which all the buckled As atoms look equally bright. For a large negative bias below −50 meV [Fig. 4(c)], a $\sqrt{2}\times\sqrt{2}$ order of bright spots is found again, which is shifted by ~4 Å with respect to the previous $\sqrt{2}\times\sqrt{2}$ order and contributed from the buckled outward As atoms. Meanwhile the

buckled inward As atoms now become almost invisible. Here a positive (negative) bias means the STM probes the states above (below) the Fermi energy. Thus the STM image can be switched from a $\sqrt{2}\times\sqrt{2}$ pattern contributed from the inward As atoms to another $\sqrt{2}\times\sqrt{2}$ pattern contributed from the outward As atoms through a 1×1 order by varying the bias voltage. In contrast, for the As-terminated surfaces of Sr122 and Ca122, neither buckling nor dimerization is found. The simulated STM images are all 1×1 ordered, similar to Fig. 4(b), even though these surfaces all take a $\sqrt{2}\times\sqrt{2}$ magnetic unit cell.

The buckling of a surface is to gain energy by lifting the degeneracy of energy band from the breaking of mirror symmetry. The buckled As atoms on the surface are partially dehybridized. This causes a charge transfer from the inward atoms to the outward ones. Consequently, the initial partially filled surface states become insulating [Fig. 1(d)]. This is the reason why the STM can observe the inward and outward atoms at a positive and negative bias, respectively. On the other hand, the buckling will cause a loss of the surface lattice distortion energy. This competing effect determines whether or not the buckling will take place. In contrast with Ba122, for both Sr122 and Ca122, no buckling is found on the As-terminated surfaces. This is because the lattice constants of both Sr122 and Ca122 are smaller than the one of Ba122 so that the lattice distortion will cost more energy than the buckling energy gain. This is similar to the buckled Si(001) surface in comparison with the nonbuckled C(001) surface. Similarly, no buckling happens on the As-terminated surfaces in the nonmagnetic tetragonal phase whereas the energy gain by the charge transfer is too small due to the strong metallicity.

In summary, our study helps establish a physical picture on cleaved $A\mathrm{Fe}_2\mathrm{As}_2$ (001) surfaces (A=Ba, Sr, or Ca). The energetically most favorable cleaved surface is of A termination with $\sqrt{2}\times\sqrt{2}$ or 1×2 order. For Ba122, the surface A atoms are found to be in a $\sqrt{2}\times\sqrt{2}$ order, in agreement with the experimental observation.[8] However, a fast cleaving at very low temperature may yield an As-terminated surface with randomly assembled A atoms as a metastable surface structure. This As-terminated surface is also found to be $\sqrt{2}\times\sqrt{2}$ ordered. This agrees with the experimental results measured by Pan and co-workers[7] for the surface structure of Ba122 cleaved at low temperature. For the As-terminated Ba122 surface, two different $\sqrt{2}\times\sqrt{2}$ STM patterns, contributed from the inward and outward As atoms respectively, can be switched by varying an applied bias. This can be used to judge whether the Ba122 surface is As or Ba terminated. This theoretical prediction can be verified by annealing an As-terminated surface to high temperatures so that the random Ba atoms can diffuse to recover a Ba-terminated surface. For the As-terminated Sr122 and Ca122 surfaces, there is no buckling, dimerization, or any other surface reconstruction. Thus the STM-observed coexistence of $\sqrt{2}\times\sqrt{2}$ and 1×2 patterns on Sr122 surface[10] should be attributed to the Sr termination. Furthermore we find that the bright spots in the 1×2 STM pattern do not directly correspond to any surface atoms. For Ca122, the Ca-terminated surface is mainly 1×2 ordered which possibly coexists partly with $\sqrt{2}\times\sqrt{2}$ order. For the As-terminated surfaces, there are surface states crossing the Fermi energy, which will affect those surface-sensitive experimental probing, for example, the Fermi-surface arcs in ARPES.

We would like to thank S. Pan for helpful discussions. This work was partially supported by National Natural Science Foundation of China and by National Program for Basic Research of MOST, China.

*zlu@ruc.edu.cn
†txiang@aphy.iphy.ac.cn

[1] Y. Kamihara, T. Watanabe, M. Hirano, and H. Hosono, J. Am. Chem. Soc. **130**, 3296 (2008).
[2] M. Rotter, M. Tegel, and D. Johrendt, Phys. Rev. Lett. **101**, 107006 (2008).
[3] C. de la Cruz, Q. Huang, J. W. Lynn, J. Li, W. Ratcliff II, J. L. Zarestky, H. A. Mook, G. F. Chen, J. L. Luo, N. L. Wang, and P. Dai, Nature (London) **453**, 899 (2008).
[4] F. Ma, W. Ji, J. P. Hu, Z.-Y. Lu, and T. Xiang, Phys. Rev. Lett. **102**, 177003 (2009).
[5] W. Bao, Y. Qiu, Q. Huang, M. A. Green, P. Zajdel, M. R. Fitzsimmons, M. Zhernenkov, S. Chang, M. Fang, B. Qian, E. K. Vehstedt, J. Yang, H. M. Pham, L. Spinu, and Z. Q. Mao, Phys. Rev. Lett. **102**, 247001 (2009).
[6] Y. Yin, M. Zech, T. L. Williams, X. F. Wang, G. Wu, X. H. Chen, and J. E. Hoffman, Phys. Rev. Lett. **102**, 097002 (2009).
[7] V. B. Nascimento, A. Li, D. R. Jayasundara, Y. Xuan, J. O'Neal, S. Pan, T. Y. Chien, B. Hu, X. B. He, G. Li, A. S. Sefat, M. A. McGuire, B. C. Sales, D. Mandrus, M. H. Pan, J. Zhang, R. Jin, and E. W. Plummer, Phys. Rev. Lett. **103**, 076104 (2009).
[8] H. Zhang, J. Dai, Y. Zhang, D. Qu, H. Ji, G. Wu, X. F. Wang, X. H. Chen, B. Wang, C. Zeng, J. Yang, and J. G. Hou, Phys. Rev. B **81**, 104520 (2010).
[9] F. Massee, S. de Jong, Y. Huang, J. Kaas, E. van Heumen, J. B. Goedkoop, and M. S. Golden, Phys. Rev. B **80**, 140507(R) (2009).
[10] F. Niestemski, Von Braun Nascimento, B. Hu, W. Plummer, J. Gillett, S. Sebastian, Z. Wang, and V. Madhavan, arXiv:0906.2761 (unpublished).
[11] P. Giannozzi *et al.*, http://www.quantum-espresso.org
[12] F. Ma and Z.-Y. Lu, Phys. Rev. B **78**, 033111 (2008).
[13] J. P. Perdew, K. Burke, and M. Ernzerhof, Phys. Rev. Lett. **77**, 3865 (1996).
[14] D. Vanderbilt, Phys. Rev. B **41**, 7892 (1990).